JOURNAL OF MATERIALS SCIENCE 6 (1971) 547–557

Some Structure-Property Relationships in Oriented Polychloroprene

E. H. ANDREWS, B. REEVE
Department of Materials, Queen Mary College, London E1

The deformation, yield and brittle fracture properties of an 84% *trans*-polychloroprene (Neoprene W) were determined at −180°C for samples prepared with a range of microstructures (including amorphous, row-nucleated and spherulitic morphologies) and a range of pre-orientations from 0 to 300%. Pre-orientation was carried out at room temperature and crystallisation, where required, at −5°C. The degree of crystallinity was low, in the region of 18%, and the crystalline morphology was monitored by thin film electron microscopy and by wide angle X-ray analysis.

The results indicate that in this temperature range a row-nucleated ("type I") morphology produces little modification of the amorphous properties at a given pre-extension except to inhibit premature fracture after yield. In contrast a distorted spherulitic ("type II") morphology, raises yield stresses and strains above those for the amorphous material and produces post-yield strain hardening not observed with the other microstructures.

In all cases, pre-orientation exerts a profound effect on elastic moduli, yield stresses and the brittle-ductile fracture transition. Some tentative mechanisms are proposed to explain these features.

1. Introduction

The influence of physical microstructure upon the mechanical properties of solids forms the basis of much current investigation and much established technology. The optimisation of properties by the manipulation of microstructure or morphology is well established practice in metallic alloys, glass ceramics, and composites.

In polymeric materials also, morphological control is frequently employed, as in the case of nucleating agents to control spherulitic size and the use of deformation in the production of polymer fibres and films. It is true to say, however, that in many such cases the microstructures have never been characterised and the optimum processing conditions have been achieved in a purely empirical manner. The idea behind the kind of work presented in this paper is that a more precise understanding of the way in which molecular orientation and crystalline morphology affect the mechanical properties of polymers might lead to further property improvements, through the conscious control of polymer microstructure.

In previous studies [1-4] crystallising elastomers have been found highly suitable for such investigations because low crystallisation rates enable them to be tested in either an amorphous or semi-crystalline condition, and because their low temperature glass transitions make it experimentally simple to put the amorphous phase into either a glassy or rubberlike state, simply by changing the temperature of test. Furthermore, a variety of different crystalline morphologies can be produced in these materials, ranging from spherulitic to fibrous, simply by holding the crystallising melt at a fixed strain.

In the present work we have used an 84% *trans*-polychloroprene to study the effect of molecular orientation and crystalline morphology on stress-strain and fracture properties at a temperature (−180°C) well below T_g in a low-crystallinity material. It is intended at a later stage to vary the degree of crystallinity also.

2. Experimental Details

2.1. Materials

The *trans*-polychloroprene used was Neoprene W

(supplied by Du Pont Co Ltd) formulated as follows:

	parts by weight
Polymer	100
ZnO	5
MgO	4
2-mercapto-imidazoline	0.35

The polymer was press-cured for 10 min at 153°C into sheets from which tensile specimens could be stamped out.

Neoprene W is a "normal" polychloroprene [5] containing 84% of *trans*,1,4(1) structural units and about 10% of *cis*,1,4(2) units. It has a narrow molecular weight distribution with a maximum around 2×10^5. The molecular weight M_c between cross-links was estimated from swelling measurements using the Flory-Rehner equation and a value of 12500 was obtained.

Using DTA, the highest observed melting temperature for the crystalline phase in unstrained polychloroprene is 35°C and the glass transition temperature for the vulcanisate is −43°C. Previous crystallisation kinetic studies [6] on bulk material indicate a maximum crystallisation rate (half-time of about 12 h) at −5°C. The maximum degree of crystallinity was determined by X-ray measurements, and was found to be 18% for the vulcanisate in question.

2.2. Thin-film Electron Microscopy

Unvulcanised films of Neoprene W were cast on the surface of water from a 2% solution in carbon tetrachloride. Films were strained if required, before collection on specimen grids, by a method similar to that used by Andrews [2] for natural rubber. The film thickness was estimated by observation of interference colours and chosen to lie in the range 800 to 1000 Å.

The films were held at temperatures in the range −30 to 30°C for times between 7 and 20 h. The crystallised specimens were transferred to the electron microscope at room temperature and observed both at very short periods in a low intensity beam and again at "normal" beam intensities. Specimen-beam interaction effects were thereby observed. Other crystallised specimens were stained with dry osmium tetroxide vapour [2] before observation.

Strained specimens of two kinds were examined, namely those extended immediately after casting and before crystallisation has had time to occur, and those allowed to crystallise in the unstrained state whilst floating on the water surface before deformation. In the former case crystallisation occurs from a strained melt (we shall call this type I morphology) whilst in the latter an established crystalline morphology is subsequently deformed (type II morphology).

2.3. Tensile Measurements at −180°

Dumbell tensile specimens, with a gauge length of 2 cm were stamped from 2 mm thick sheets of vulcanisate. Morphological variations were introduced by using specimens in the following conditions.

(*a*) As cut from the sheet and thus possessing a spherulitic morphology.

(*b*) After pre-orientation at room temperature to 100, 200 and 300% strain, thus containing distorted spherulites (type II morphology).

(*c*) After pre-orientation as in (*b*) followed by melting under strain (in a vacuum oven at 70°C for 2 h) and crystallisation, still under strain, at −5°C for not less than five days. This produces crystallisation from a strained melt, i.e type I morphology.

(*d*) After pre-orientation and melting, but quenched to −180°C for tensile testing before significant crystallisation could occur. This provides an amorphous reference material.

Since earlier work by Reed [3] had shown that crystalline morphology exerts its greatest effect upon ultimate properties in *cis*-polyisoprene when the amorphous phase is glassy (i.e. below T_g), tensile testing was carried out at −180°C. An Instron testing machine was used in conjunction with the cryostat designed by Reed [7], and a period of 30 min was allowed for specimens to equilibrate at temperatures before testing commenced. Strain rates from 10 to 0.005 cm/min were employed.

2.4. Wide Angle X-ray Diffraction

To supplement the characterisation of morphologies obtained by thin-film electron microscopy, wide angle transmission X-ray studies were carried out on bulk specimens prepared in an identical manner to those for tensile testing. this will be discussed further in the Results section.

3. Results and Discussion

3.1. Electron Microscopical Data

The comparison between unstained specimens "before" and after electron irradiation showed firstly that the visual structure was real and not an artefact of electron beam damage, although

micrographs taken after irradiation showed a less distinct structure, as if partial melting had occurred. Electron diffraction of unstained samples at room temperature under low intensity conditions confirmed that the crystallinity is quickly destroyed. These results are completely analogous to Andrews' results on natural rubber [1]. As in the natural rubber work, this problem of beam damage was overcome by staining with osmium tetroxide. It was established that a 20 sec stain in the vapour efficiently fixes the structure and prevents further crystallisation, although, of course, electron diffraction can no longer be used. This procedure having been established, the development of crystallinity with time in unstrained films was studied. The expected sequence in this development was always observed, namely the formation of crystalline lamellae (or filaments), bundles, sheaf-like aggregates and finally the spherulite itself. Fig. 1a shows a film with well developed sheaf-like aggregates; considerable twisting and intertwining of the fibrils from the central nucleus region is apparent. A fully crystallised spherulitic film with well defined spherulite boundaries, and a range of spherulite shapes and size is presented in fig. 1b; this two-dimensional spherulite array can be considered analogous to the three-dimensional spherulite structure to be found in bulk crystallised material such as used for tensile testing.

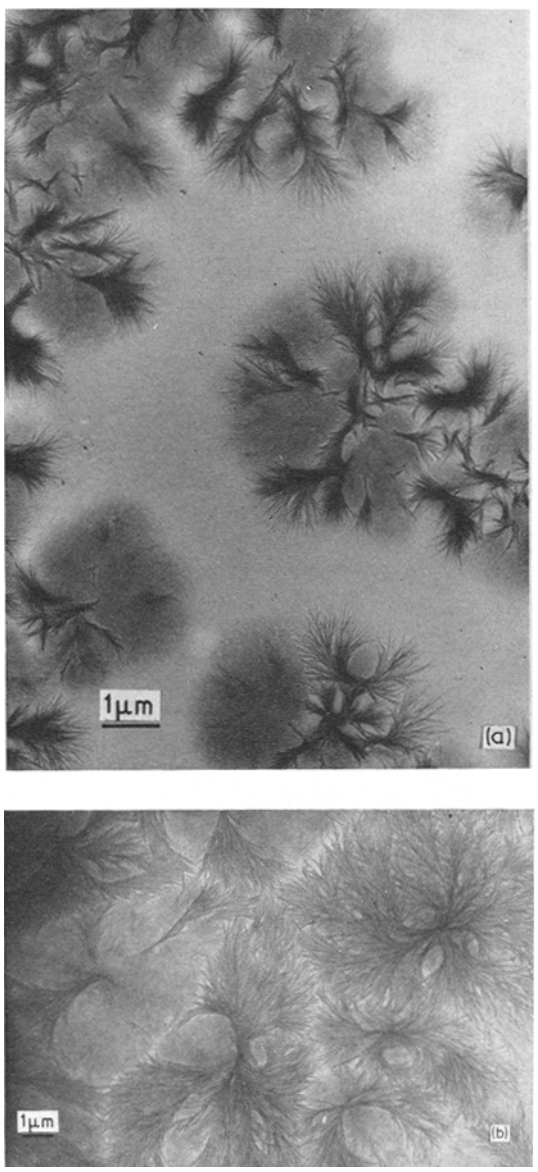

Figure 1 (a) Thin film of polychloroprene partially crystallised unstrained at −5°C, unstained. (b) As fig. 1a but fully crystallised.

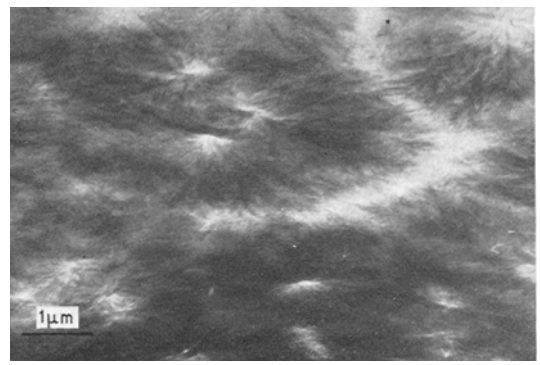

Figure 2 Distorted spherulites in film crystallised before straining by 200% at room temperature (Type II morphology).

Deformation of a spherulitic film should result in the initially spherical spherulites being deformed into ellipsoidal shapes (our type II morphology). As can be seen from fig. 2 this is the case, the ellipsoidal character growing more marked as the elongation is increased. A variation in spherulite elongation in different regions of the film was observed, this localised deformation agreeing with the optical observations of Gorbunov [8] on Nairit NP chloroprene rubber. However, in applying these findings to equivalent deformations in bulk specimens, it will be assumed that such variations are absent, since they probably arise from thickness variations in the film.

The basic feature of samples crystallised under

strain (type I morphology) was the development of a fine fibrous texture perpendicular to the direction of strain. Comparisons will be made for films stretched and crystallised at the strains used in the tensile tests, that is 100, 200 and 300% Fig. 3a shows the typical early stages of crystallisation for 100% films. These row nucleated structures are very similar to those found by Andrews [2] in natural rubber, with α-filaments growing perpendicular to the strain axis, and

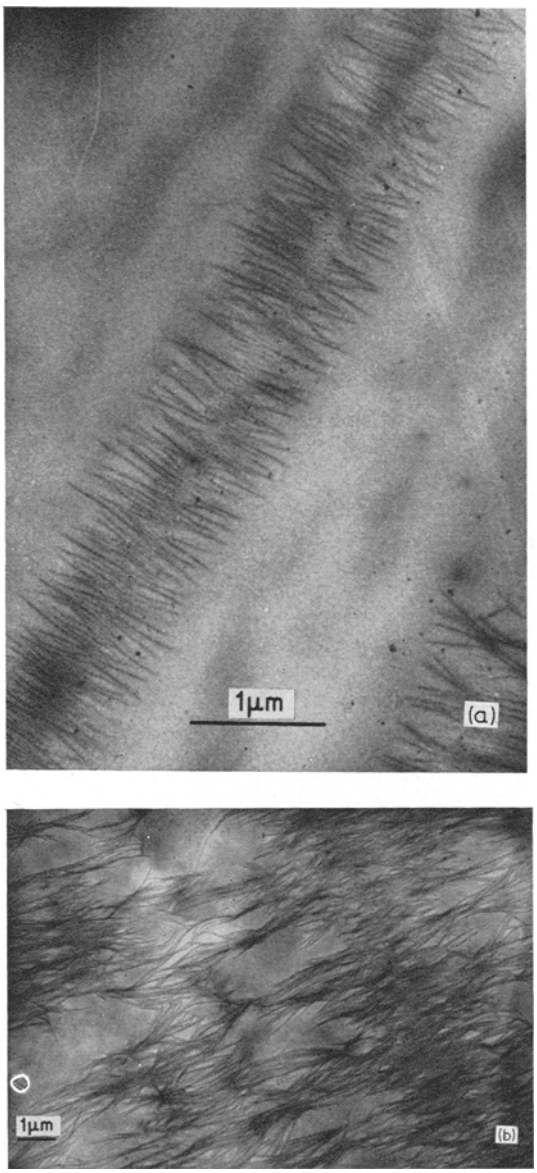

Figure 3 (a) Thin film of polychloroprene partially crystallised under 100% strain at −5°C. Stained OsO_4. (b) As fig. 3a but fully crystallised.

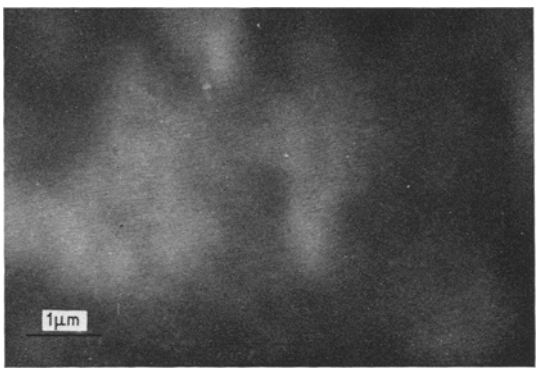

Figure 4 Film fully crystallised under 400% strain at −5°C. Stained OsO_4.

appear to be a general feature of crystallisation from a strained polymer melt, as proposed by Keller and Machin [9]. At a later stage (fig. 3b) the fibrils diverge and intertwine with adjacent row structures. The effect of increasing the elongation to 200% is to increase the nucleation density (i.e. the proportion of "γ-filaments") while decreasing α-filament separation distance and inhibiting α-filament length. This is illustrated in fig. 4 which shows a fully crystallised film at 200% strain. At still higher elongations the crystallinity is predominantly composed of γ-filaments with negligible α-filament growth. Finally, figs. 5a, b and c, are presented as evidence for the existence of a central nucleating thread. Figs. 5a and b represent 100 and 200% elongated films respectively, and close inspection of the nuclei indicates a particulate nature. This is highlighted in fig. 5c for a film stretched 800% where γ-filaments only are generated spontaneously. In a particularly thin part of the film there is a profusion of closely spaced aligned filaments, which possess a particulate structure, approximately diamond-shaped with dimensions varying from 250 to 300 Å in each direction. The role played by strain in the formation of these filaments suggests that they may consist of a "hidden", extended chain, central thread with an overlay of chain folded growth to produce the observed particulate appearance. They would then be analagous both to the intercrystalline links observed by Keith *et al* [10] and to the early stages of crystallinity in stirred polymer solutions [11]. Owen has obtained electron micrographs from strained natural rubber which show clearly a central crystalline thread, from which folded-chain lamellae are being nucleated and was able to melt off the lamellae leaving only

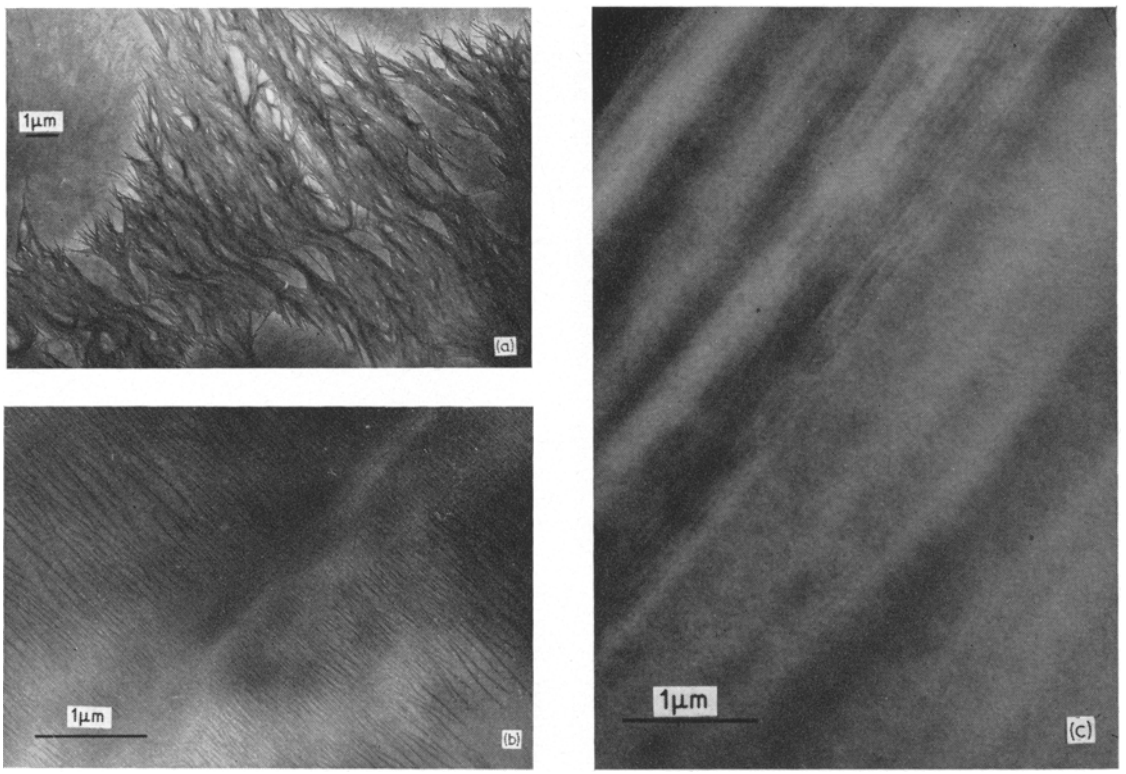

Figure 5 (a) Crystallisation under 100% strain showing nucleating backbone thread. (b) Nucleating backbone in film crystallised under 200% strain. (c) Nucleating threads in a film stretched to 800%.

the central thread which measures as little as 30 Å in diameter [12].

The assumption that the observed thin film morphologies are characteristic of those in similarly prepared bulk specimens is enhanced by the recent work of Yoshimoto *et al* [13]. They have reported micrographs from thin sections of a polychloroprene with a 30% degree of crystallinity. They did not directly section the bulk material, but first prepared a film (of unspecified thickness), stained this in osmium tetroxide vapour for three days, and then thin-sectioned the film. The structures obtained are equivalent to the unstrained morphology reported in this investigation. In our own studies, lamellar structures have been observed with some difficulty in ultrathin sections cut at low temperature and stained with OsO_4 (fig. 6).

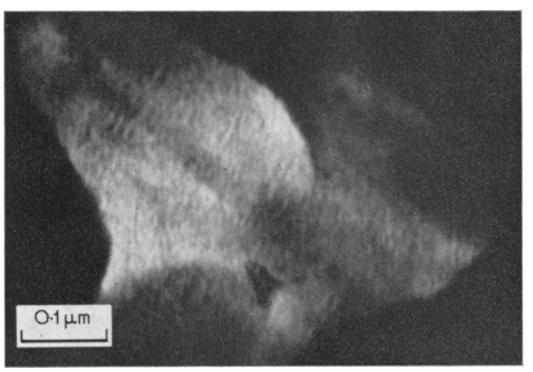

Figure 6 Lamellar structure revealed in an ultrathin section cut at low temperature and stained with OsO_4.

3.2. Wide Angle X-ray Diffraction

A determination of orientation functions cannot characterise the morphology as fully as direct electron microscopical observation, but since the latter method is open to the criticism that thin films may crystallise differently from bulk material, any supplementary data on bulk morphology is useful. The technique was also used to establish the temperature and period of heating required to melt the crystallites in the elongated specimens prior to recrystallisation in the strained condition. Fig. 7 shows diffraction

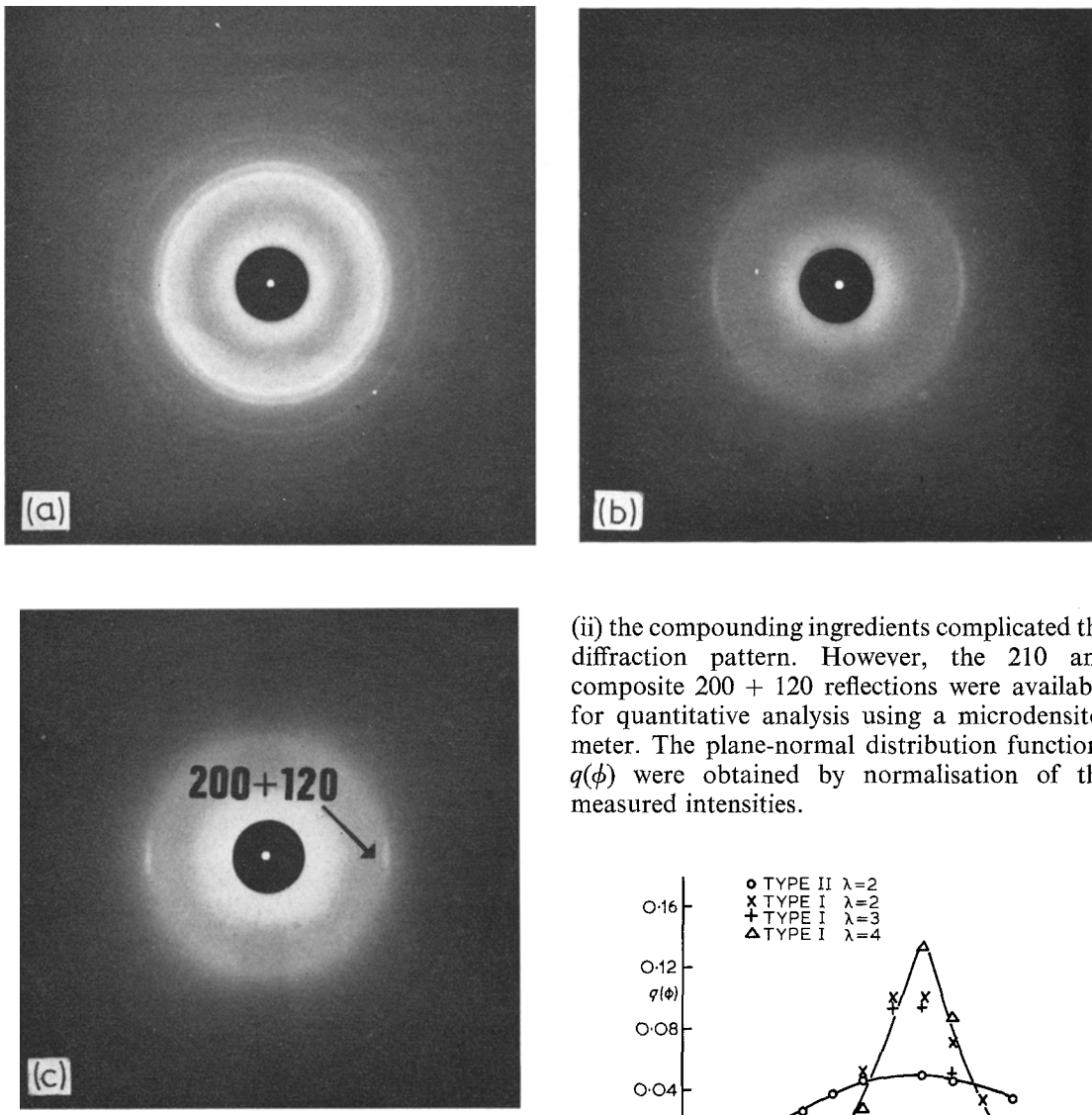

Figure 7 Wide angle X-ray diffraction patterns for (a) unoriented raw polychloroprene. (b) vulcanisate, crystallised and strained to $\lambda = 2$ (type II morphology). (c) vulcanisate, crystallised under strain at $\lambda = 2$ (type I morphology).

patterns for the raw rubber, and for the vulcanised rubber in the various conditions subsequenty used for tensile tests. The reflections were indexed using the orthorhombic unit cell dimensions $a = 8.84$, $b = 10.34$, and $c = 4.79$ Å [14]. Two things were immediately apparent: (i) in contrast to other reported studies [15] the c-axis orientation could not be monitored directly because the 002 reflection at $\tan 2_\theta = 37.60°$ was missing or too weak to detect, and (ii) the compounding ingredients complicated the diffraction pattern. However, the 210 and composite 200 + 120 reflections were available for quantitative analysis using a microdensitometer. The plane-normal distribution functions $q(\phi)$ were obtained by normalisation of the measured intensities.

Figure 8 Plane normal distribution function $q(\phi)$ for the composite (200) + (120) reflection for different extension ratios and morphologies.

These functions, from the composite 200 + 120 reflection, are plotted against ϕ in fig. 8 for (a) type II morphology at extension ratio $\lambda = 2$ and (b) type I morphology also at $\lambda = 2$, but with results for $\lambda = 3$ and 4 also included. The c-axis is the chain direction of the polychloroprene molecule and since the normals to the 200 and 120 planes are perpendicular to the c-axis, it is apparent from fig. 8 (where the

distribution function has a peak at $\phi = 90°$) that the crystallites in both morphologies align with the *c*-axis in the stretching direction. Krigbaum *et al* [15] obtained similar results in their detailed diffraction study of stretched Neoprene HC film (type I morphology). It was also found that the 210 plane normal distribution function curve was very similar to that of the 200 + 120 case, indicating, as Krigbaum *et al* also suggest, that the crystallites orient randomly around the *c*-axis.

Although there are, therefore, qualitative similarities between the results for type I and type II specimens, the quantitative differences are strongly apparent. A far greater *c*-axis alignment is achieved in type I morphologies for a given extension ratio, and this alignment is achieved at relatively low λ, with little further increase as λ rises from 2 to 4. In contrast, the *c*-axis alignment in type II specimens increases progressively with increasing λ.

These results are in excellent agreement with the thin film morphologies in which row nucleation produces a highly aligned crystalline texture in type I morphologies at the relatively low λ of 2, whereas the type II morphology results from the progressive deformation of an initially spherical lamellar array, the lamellae probably orienting by the combined processes of tilt and slip on (hk0) planes and achieving only moderate *c*-axis orientation at low λ.

These data therefore strengthen the assumption that the morphologies in bulk material correspond closely to those in thin films prepared under the same conditions of strain.

3.3. Mechanical Properties

3.3.1. Stress-Strain Curves

In these data "stress" is the engineering stress, i.e. based upon initial cross-section area, and "strain" is a nominal figure derived from the cross-head movement assuming that, at these low temperatures, the deformation occurs only in the gauge-length of the dumbell specimen. The straining rate is always plotted logarithmically so that it is sufficient for our purpose to plot log (crosshead speed) instead of the log (strain rate proper).

Typical stress-strain curves are shown in figs. 9, 10 and 11. These curves are for a crosshead speed of 0.2 or 0.5 cm/min although the curves are not greatly affected by strain-rate except in one important respect; the ductile or brittle behaviour.

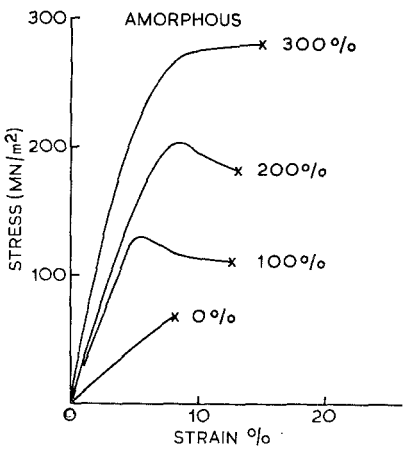

Figure 9 Stress-strain curves for oriented amorphous material at −180° C.

The curves for amorphous material at −180° C are shown in fig. 9. The 0% specimens are brittle (except at very low strain rates), but oriented material yields, before fracturing at relatively low extensions of 13 to 15%. This early post-yield fracture is characteristic of the amorphous material.

Both initial modulus and yield stress increase strongly with pre-orientation, a sevenfold increase in modulus occurring as this rises from 0 to 300%. This is a far greater increase than observed in a typical glassy polymer, PVC, tested at room temperature. Gibbs [16] observed a modulus rise of only 35% as pre-orientation varied over the same range of 0 to 300%.

Fig. 10 shows data for type I (row nucleated) morphology. These curves are surprisingly similar in their initial regions to those for amorphous material, both the moduli and yield stresses being very similar at corresponding pre-extensions. The row nucleated material was, however, highly ductile under most conditions, giving plastic extensions to break in excess of 50%, except for the 0% material, which was brittle. This ductility was associated with the formation and growth of white striations in the gauge length which "foamed" on warming to room temperature in the manner reported by Andrews and Reed for natural rubber [17]. The details of the foaming phenomenon, together with an ESR study of free radical production during testing will be published elsewhere, but it has been convincingly demonstrated that the whitened portions are regions of micro-voiding,

i.e. a kind of crazing which is not limited to a geometrically narrow band.

It appears, therefore, that the row nucleated (type I) morphology differs from oriented amorphous material chiefly in its capacity to accept micro-void formation without specimen fracture. The crystalline row structure probably inhibits crack propagation either by a fibre-reinforcement mechanism or else by the enhancement of local ductility at the tip of a potentially catastrophic crack. This enhancement could result from crystallographic slip within the lamellae.

Results for type II morphologies are given in fig. 11. The 0% curve is, of course, the same as for type I specimens, but specimens with pre-extensions behave quite differently to their row-nucleated counterparts.

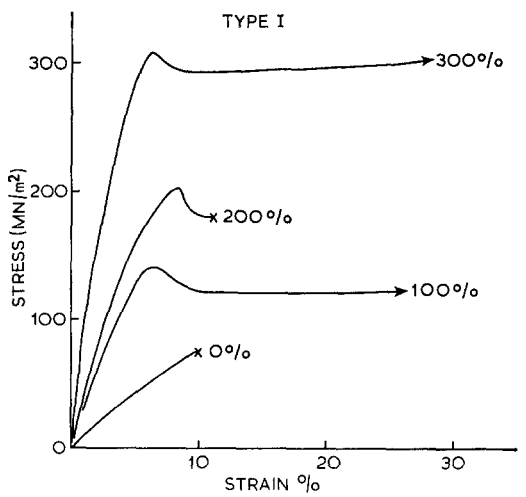

Figure 10 Stress-strain curves for type I morphologies at −180° C.

The initial moduli are similar for both morphologies at corresponding pre-extensions suggesting that these are determined by average molecular orientation rather than by morphology as such. The yield stresses are, however, higher for type II specimens, the amounts varying from nearly 30% at 100% pre-extension to zero at 300%. Yield strains for type II are also higher, the yield strain being doubled for 100% pre-extension, but similar to type I and amorphous specimens at higher pre-extensions. Most obviously, immediate post-yield strain hardening is found for type II morphologies at pre-extensions of 200% or more, and fracture strains are large (> 30%). Post yield foaming occurs at low strain rates in the type II specimens but not

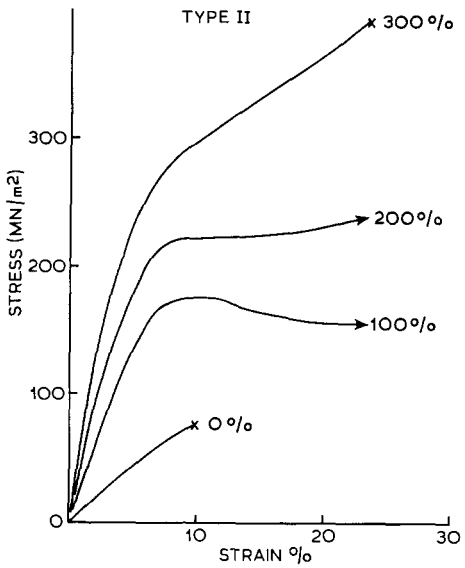

Figure 11 Stress-strain curves for type II morphologies at −180° C.

at high pre-extension. This suggests that micro-void formation is less readily achieved in type II morphologies and this in turn could explain the strain hardening.

3.3.2. *Yield Stresses and the Brittle-Ductile Transition*

Data for yield or brittle fracture stresses (σ_y or σ_B) as a function of testing speed is plotted in figs. 12, 13 and 14. Yield is denoted by open circles and brittle behaviour by the filled points, transitional behaviour being indicated by a half-filled circle.

All materials reveal an increase in σ_y or σ_B with pre-extension, a factor of between four and six existing between 0 and 300% pre-extensions in all morphologies. At a given pre-extension the effect of rate on σ_B is negligible, but σ_y increases slowly with strain rate in a manner apparently independent of the morphology. It appears that the time dependence of the yield stress is determined only by the visco-elastic response of the amorphous phase.

The brittle-ductile transition speed at −180° C is marked on the graphs by an arrow and is shown more explicitly in fig. 15. There is an approximately linear dependence of the log (transition speed) upon the pre-extension, the data for amorphous and row-nucleated morphologies being indistinguishable. The curve for type II morphology shows that pre-strain is

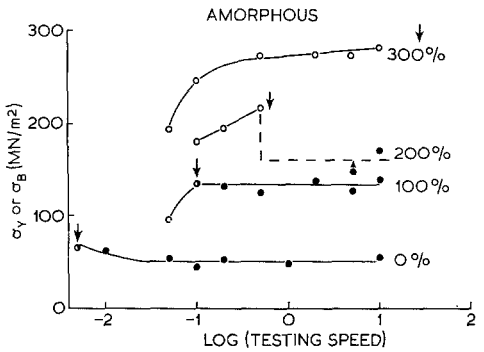

Figure 12 Yield or brittle stress data for amorphous material at −180°C. Arrows show brittle-ductile transition speed.

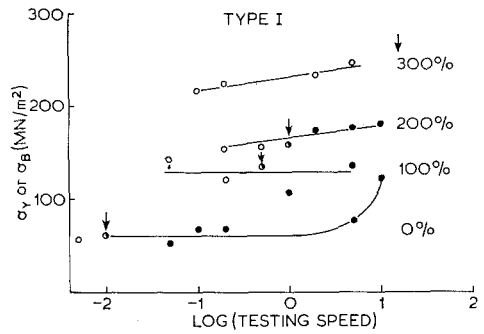

Figure 13 As fig. 12 but for type I morphologies.

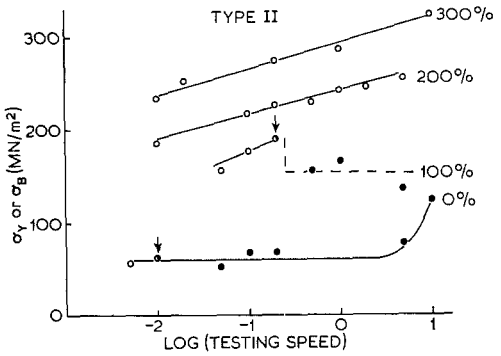

Figure 14 As fig. 12 but for type II morphologies.

relatively more effective in suppressing brittle behaviour than with amorphous or type I structures.

3.4. Discussion

The documentation of structure-property relationships constitutes the necessary first-step in explaining the mechanical behaviour of semi-crystalline polymers. The data presented in this paper is of a documentary nature and it would

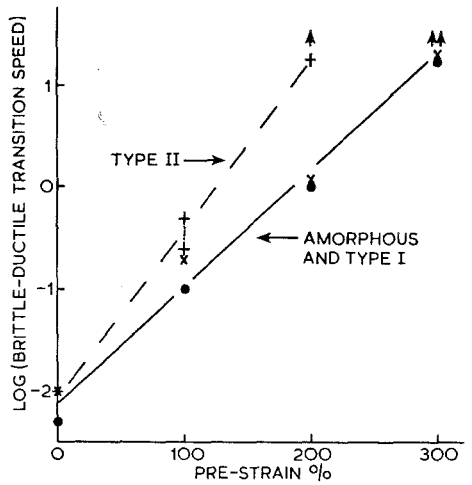

Figure 15 Brittle-ductile transition as a function of orientation.

be premature to attempt any detailed mechanistic interpretation.

What has been shown, however, is that the mechanical properties of a semi-crystalline polymer are significantly affected by morphology even at low degrees of crystallinity. That the morphology, rather than the absolute degree of crystallinity, is significant follows from the close similarity in many respects of row-nucleated and amorphous materials in contrast to the type II (deformed spherulitic) material. If anything, type I morphologies should be more highly crystalline than spherulitic polymer, yet it is the latter which behaves differently.

By "morphology", of course, we mean more than the basic geometrical arrangement of crystalline and amorphous phases. In differentiating between type I and type II morphologies for example we must recognise not only the difference in average *c*-axis alignment revealed by X-rays and electron microscopy, but also the "invisible" differences. These include the room temperature distortion of lamellae, involving crystallographic slip and possible cold work, and the complex state of strain of the amorphous phase between lamellae (including any tie-molecular network) which effects are absent in type I morphologies. It is probably to these hidden causes that the major differences observed should be attributed, since the greater *c*-axis alignment of type I would otherwise be expected to make *this* morphology exhibit the most distinctive behaviour, contrary to observation.

To come to details, the major effects of morphology were found to be as follows:
(1) The only significant difference between amorphous and row-nucleated materials is the ability of the latter to undergo large post-yield deformations. This in turn appears to reflect the ability of row nucleated structures to withstand extensive micro-void formation without failure. This would be explained if the micro-voids were prevented from linking up into a crack, possibly because the row structures act like fibre reinforcement, or because the micro-void walls strain-harden on account of crystallographic slip (leading to cold work) in the crystalline phase. In all other respects the stress-strain behaviour at $-180°C$ of these two materials is governed by the overall alignment of the molecules imposed at 20°C. This implies that such properties as elastic modulus and yield stress in these materials are governed by the amorphous glassy phase.
(2) Type II (distorted spherulitic) material differs in several important respects. At intermediate pre-strains the yield stress and strain were elevated in comparison with amorphous and type I materials. This is attributed to the higher residual strain in the amorphous phase of type II material. At a given pre-strain ϵ_0 the amorphous phase in type II must have an average resolved strain at least equal to ϵ_0 and possibly greater, depending on the deformability of the crystalline phase. In type I morphologies the residual strain in the amorphous phase relaxes during crystallisation, so is less than ϵ_0. Some regions in type II (e.g. any tie molecules between lamellae) will be highly oriented. It is suggested that the higher-than-nominal amorphous orientation in type II morphologies has the effect of raising the yield stress, in harmony with the increase found with pre-orientation in the purely amorphous material. As pre-strain increases, this effect would be minimised as the amorphous orientation in all three types of material increases to a high level.

The second noticeable difference displayed by type II material is its immediate post-yield strain-hardening at the higher pre-extensions. Since deformation at constant load in amorphous and type I material is caused by micro-void formation, this behaviour points to an inhibition of void formation or growth. Studies of void formation in glassy polymers [18] show that local strain-hardening in the walls of a growing void would have just such an effect. A higher local strain-hardening rate would be expected of type II material both on account of the higher residual amorphous strain and of any prior cold-work in the crystalline phase during pre-extension.

The greater effectiveness of pre-strain in preventing brittle fracture in type II materials (see fig. 15) can be explained in similar terms. Rapid strain-hardening, either associated with the onset of micro-voiding or even the propagation of a normal brittle crack, would inhibit brittle behaviour.

4. Conclusion

Under some circumstances the morphology of a semi-crystalline polymer can exert a greater influence on mechanical properties than the degree of crystallinity itself, and this effect is observable even in a polymer having overall crystallinity as low as 18%. Most of the explanation appears to lie in the state of strain of the amorphous phase, including any tie molecular network which may exist, and in its strain-hardening propensity. Yield and flow phenomena in the materials tested and at the low temperature employed appear to be governed by a generalised micro-cavitation and such resistance to cavity growth as the material might display. Resistance to cavity coalescence probably also controls brittle-ductile transition phenomena and plastic extensibility.

Acknowledgements

The authors would like to thank Mr V. N. Chatterton of the Du Pont Company for furnishing the Neoprene compound, Dr F. R. Martin for practical help and valuable discussions concerning the X-ray diffraction studies, and Mr R. L. Whitenstall for the processing of the micrographs. One of us (B.R.) is grateful to the Science Research Council for financial support.

References

1. E. H. ANDREWS, *Proc. Roy. Soc.* **A270** (1962) 232.
2. *Idem, ibid* **A277** (1964) 562.
3. P. E. REED, Ph.D. Thesis, "The influence of crystalline texture on the tensile properties of natural rubber" (University of London, 1970).
4. E. H. ANDREWS, *New Scientist*, **42** (1969) 360.
5. J. T. MAYNARD and W. E. MOCHEL, *J. Polymer Sci.* **18** (1955) 227.
6. V. GOMELA and L. MEGARSKAYA, *Polymer Sci. USSR* **10** (1968) 1196.
7. P. E. REED, *J. Mater. Sci.* **1** (1966) 91.
8. P. M. GORBUNOV, *Polymer Sci. USSR* **11** (1969) 436

9. A. KELLER and M. J. MACHIN, *J. Macromol. Sci. (Phys.)* **B1** (1) (1967) 41.
10. H. D. KEITH, F. J. PADDEN, and R. G. VADINSKY, *J. Appl. Phys.* **37** (1966) 4027.
11. A. J. PENNINGS and A. M. KIEL, *Kolloid-Z.* **205** (1965) 160.
12. P. J. OWEN, Ph.D. Thesis, "Crystallization in Thin Films of Natural Rubber" (University of London, 1970).
13. H. YOSHIMOTO, S. SAGAE, M. MATSUO, S. VEMURA and Y. ISHIDA, *Kolloid-Z.* **236** (1970) 116.
14. C. W. BUNN, *Proc. Roy. Soc.* **180A** (1944) 41.
15. W. A. KRIGBAUM, J. V. DAWKINS, and G. H. VIA, *J. Polymer Sci.* **A2, 7** (1969) 257.
16. H. G. GIBBS, Thesis, "The tensile failure of uniaxially oriented unplasticised PVC" (The College of Aeronautics, Cranfield, 1966).
17. E. H. ANDREWS and P. E. REED, *J. Polymer Sci.* B (Polymer Letters) **5** (1967) 317.
18. E. H. ANDREWS and L. BEVAN, to be published.

Received 14 January and accepted 15 March 1971.